Evolution of the oligotrophic West Pacific Warm Pool during the Pliocene

Himanshu Bali[1], Anil K Gupta[2], Kuppusamy Mohan[3], Kaustubh Thirumalai[4], Sameer K Tiwari[5], and Mruganka K Panigrahi[6]

[1]IIT Kharagpur
[2]Indian Institute of Technology, Kharagpur
[3]VIT University Chennai Campus
[4]University of Arizona
[5]Wadia Institute of Himalayan Geology
[6]Indian Institute of Technology Kharagpur

November 23, 2022

Abstract

This study investigates the timing of development of the oligotrophic conditions and thickening of the West Pacific Warm Pool (WPWP) during the Pliocene. It has been hypothesized that the evolution of the WPWP and the establishment of equatorial Pacific zonal gradients are closely related to the narrowing of the Indonesian seaway (IS) as well as the closure of the Panama gateway; however, the timing of these events remain debated. Here we analysed planktic foraminiferal abundances combined with stable oxygen and carbon isotope ratios since the Pliocene at ODP Hole 807A, western Pacific and DSDP Site 214, eastern Indian Ocean. A comparison of the population of mixed-layer species (MLS) from both study sites shows a significant increase between ~3.15 and 1.6 Ma. On the contrary, shows a decrease in its population during this time, indicating oligotrophic conditions in the western tropical Pacific. The dC ratio of epibenthic foraminiferal species shows a decreasing trend from ~3.15 to ~2.0 Ma, indicating the lowering of productivity during this interval. Our data suggest that the WPWP developed ~3.15 Ma and was closely linked to the gradual closure of the IS.

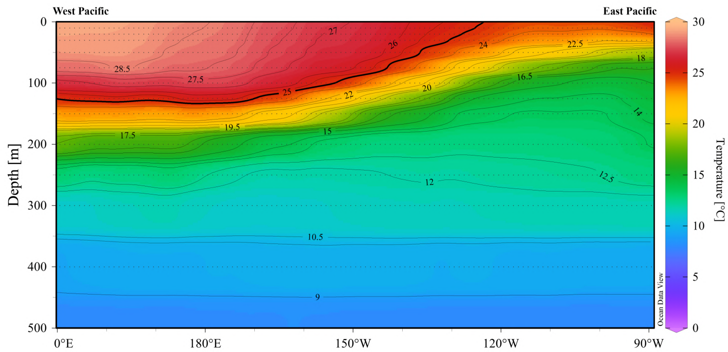

Figure 2: Average ocean surface temperature along the equator in the Pacific.
Background was created using Ocean-Data-View (Schlitzer, 2014).

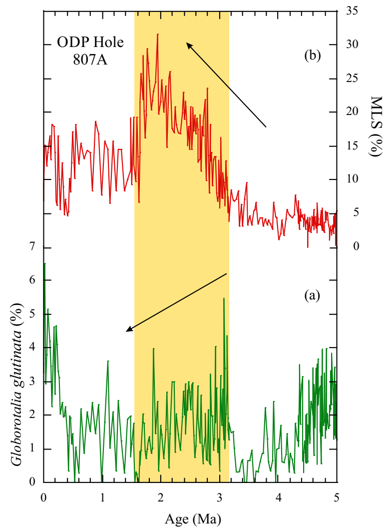

Figure 4: Percentage distribution of *Globorotalia glutinata* (a), % Mixed layer Species (b) at ODP Hole 807A.

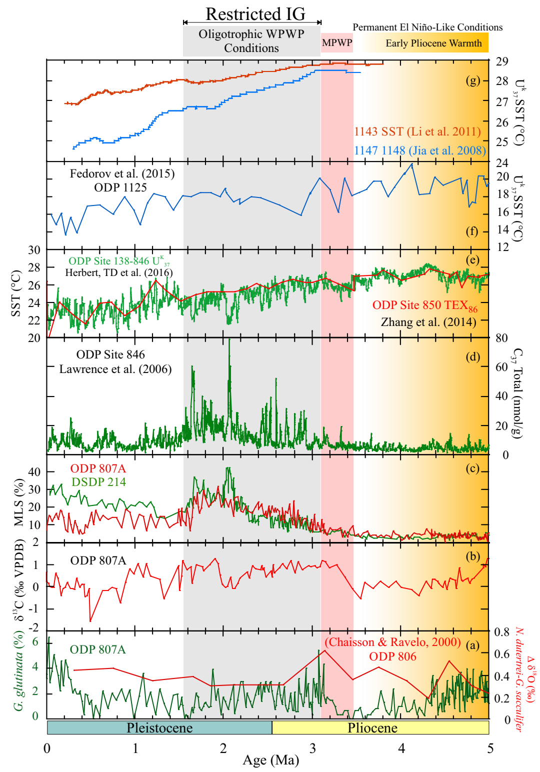

Figure 5: Proxy records at ODP Hole 807A compared with those from the other sites. (a) Percentage distribution of *Globigerinita glutinata* (present study) and The $\delta^{18}O$ differences ($\Delta\delta^{18}O$ values) between *Globigerinoides sacculifer* (surface) and *Neogloboquadrina dutertrei* (thermocline) dwellers at ODP Site 806 (Chaisson and Ravelo, 2000) (red), (b) $\delta^{13}C$ values of *Cibicides wuellerstorfi* and *Cibicides kullenbergi* at ODP Hole 807A present study), (c) % Mixed-layer species at ODP Hole 807A and DSDP Site 214 (present study), (d) Concentration of alkenones C_{37} Total (nmol/g) at ODP Site 846 (Lawrence et al., 2006). (e) SST based on U^{k}_{37} at ODP Site 138-846 U^{k}_{37} (Herbert, TD et al., 2016) (green) and SST based on TEX_{86} at ODP 850 (Zhang et al., 2014) (red), (f) SST based on U^{k}_{37} at ODP Site 1125 (Fedorov et al., 2015), (g) SST based on U^{k}_{37} at ODP Site 1143 (Li et al., 2011) and at ODP Site 1147/1148 (Jia et al., 2008). IG = Indonesian Gateway; WPWP = West Pacific Warm Pool; MPWP = Mid-Pliocene Warm Period.

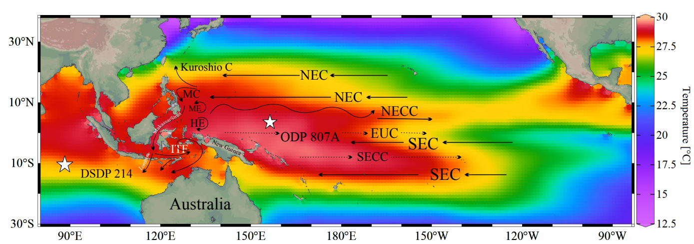

Figure 1: Location of ODP Hole 807A and DSDP Site 214. Background was created using Ocean-Data-View (Schlitzer, 2014). NEC = North Equatorial Current; NECC = North Equatorial Countercurrent; SEC = South Equatorial Current, SECC = South Equatorial Countercurrent; EUC = Equatorial Undercurrent; MC = Mindanao Current; ME = Mindanao Eddy; HE = Halmahera Eddy.

Evolution of the oligotrophic West Pacific Warm Pool during the Pliocene

Himanshu Bali[1], Anil K. Gupta[1*], Kuppusamy Mohan[2], K. Thirumalai[3], Sameer K Tiwari[4], Mruganka K. Panigrahi[1]

[1] Department of Geology and Geophysics, Indian Institute of Technology, Kharagpur 721302, India

[2] School of Mechanical and Building Sciences, VIT University Chennai Campus, Chennai, 600127, India

[3] Department of Geosciences, University of Arizona, Tucson, AZ 85721

[4] Wadia Institute of Himalayan Geology, Dehradun 248001, India.

*Corresponding author: anilg@gg.iitkgp.ac.in

Key Points:

- Evolution of the western Pacific surface paleoceanography during the Pliocene
- Linkages between evolution of West Pacific Warm Pool and shrinking of Indonesian seaway
- The oligotrophic West Pacific Warm Pool began to develop at ~3.15 Ma

Abstract

This study investigates the timing of development of the oligotrophic conditions and thickening of the West Pacific Warm Pool (WPWP) during the Pliocene. It has been hypothesized that the evolution of the WPWP and the establishment of equatorial Pacific zonal gradients are closely related to the narrowing of the Indonesian seaway (IS) as well as the closure of the Panama gateway; however, the timing of these events remain debated. Here we analysed planktic foraminiferal abundances combined with stable oxygen and carbon isotope ratios since the Pliocene at ODP Hole 807A, western Pacific and DSDP Site 214, eastern Indian Ocean. A comparison of the population of mixed-layer species (MLS) from both study sites shows a significant increase between ~3.15 and 1.6 Ma. On the contrary, *Globigerinita glutinata* shows a decrease in its population during this time, indicating oligotrophic conditions in the western tropical Pacific. The $\delta^{13}C$ ratio of epibenthic foraminiferal species shows a decreasing trend from ~3.15 to ~2.0 Ma, indicating the lowering of productivity during this interval. Our data suggest that the WPWP developed around ~3.15 Ma and was closely linked to the gradual closure of the IS.

Keywords: West Pacific Warm Pool, planktic foraminifera, Pliocene, Mixed-layer species, oxygen and carbon isotopes, Indonesian seaway.

1. Introduction

The West Pacific Warm Pool (WPWP) encompasses most of the tropical–subtropical area (>30 × 10^6 km^2) of the western Pacific (Cane and Molnar, 2001) and is characterized by warm surface waters with an annual sea-surface temperature (SST) of >28°C (Yan et al., 1992; Webster and Palmer, 1997) (Fig. 1). The WPWP is ~2–5°C warmer than any other equatorial region and stores large amount of heat (Yan et al., 1992). Thus any change in the size and temperature of the WPWP affects global heat transport from the equator to poles and also play a role in the evolution of El-Niño-Southern Oscillation (ENSO) events (Meyers et al., 1996; Sun, 2003; de Garidel-Thoron et al., 2005). Easterly trade winds keep the WPWP towards the western equatorial Pacific (WEP) under normal conditions (Li et al., 2006), although its position fluctuates during ENSO events. Oceanographically, the WPWP is composed of a thick and warm mixed-layer with a consequently deep thermocline (~200 m) that contrasts with the eastern equatorial Pacific (EEP), which contains a shallow thermocline and smaller mixed-layer (Fig. 2). This tilt in the thermocline makes the eastern Pacific more productive than the West (Ravelo et al., 2006). About 10–15 Sv (1 Sv=10^6 m^3s^{-1}) of low-salinity, warm water enters the eastern Indian ocean from the WPWP annually (Chong et al., 2000; Ganachaud and Wunsch, 2000) and is termed the Indonesian Throughflow (ITF). The ITF transports heat from the WEP north of the equator to 12°S into the eastern Indian Ocean, mostly through the Makassar Strait (Gordon et al., 1999), and varies on annual, interannual, and (multi-)decadal timescales (Linsley et al., 2010). Variability in the ITF thus influences global climates on both short (El-Niño-Southern Oscillation or ENSO-related) and long-term or tectonic timescales (Schott and McCreary, 2001). Observations indicate that fluctuations in ENSO and related changes in the Indian monsoon system are linked to major influxes of Pacific freshwater and heat into the Indian Ocean (Vranes et al., 2002), wherein ITF transport is greater during La-Niña events compared to El-Niño events. (Gordon and Fine, 1996).

2. Evolution of the West Pacific Warm Pool (WPWP)

Small changes related to the dimensions of the oceanic seaways can influence ocean circulation and heat distribution, and may therefore have a profound impact on the global climate and ocean productivity (Cane and Molnar, 2001; Nathan and Leckie, 2009). Progressive narrowing of the Indonesian seaway (IS) is purported to have played a key role in altering and redirecting ocean currents and causing climate change in the tropical eastern Indian and western Pacific Oceans. Numerous investigations have hypothesized that the constriction and closure of the IS, the closure of the Panama gateway, and the development of the WPWP are closely linked (Keller, 1985; Kennett et al., 1985; Chaisson and Ravelo, 2000; Jian et al., 2006; Li et al., 2006; Nathan et al., 2009). Kennett et al. (1985) and Keller (1985) used planktic foraminiferal faunal abundance and isotopes to investigate surface and subsurface circulation changes in the equatorial Pacific, including the Equatorial Under Current (EUC) over the Miocene. These studies found a gradual shoaling of the EUC towards the EEP over the past 10 Myr, and concluded that this was due to the narrowing of the IS and subsequent closure of the Panama gateway. Chaisson and Ravelo (2000) used planktic foraminiferal data from the WEP and EEP to suggest that the east–west thermocline tilt developed in the equatorial Pacific during 4.5 to 4 Ma and was related to the closure of the Panama gateway. Contrastingly, Jian et al. (2006) posited a much earlier formation of the WPWP using planktic foraminiferal records in the South China Sea and related it to the closure of the IS during 11.5 to 10.6 Ma.

Studies of climate simulations also provide disparate answers regarding the timing of the development of the WPWP. Model results from Cane and Molnar, (2001) have suggested that the northward movement of New Guinea during the Pliocene, which effectively prevents the transport of warm, saline South Pacific waters into the Indian Ocean, is key to the establishment of the WPWP. On the other hand, Nathan et al. (2009) have shown that decreasing sea-level around 11-10 Ma led to the development and intensification of the WPWP. Results based on multi-species foraminiferal isotopic analyses and assemblages of equatorial Pacific deep-sea cores suggest the evolution of the modern WPWP after ~3.6–3.0 Ma in the Pliocene (Chaisson, 1995; Cannariato and Ravelo, 1997; Chaisson and Ravelo, 2000; Ravelo et al., 2006; Sato et al., 2008). Therefore, despite significant progress in the understanding of closure of the IS and evolution of the WPWP, the timing of the tectonic constriction of the IS still remains debatable with estimates of age ranging from ~17 to 3 Ma (Kennett et al., 1985; Jian et al., 2006; Li et al., 2006).

Here we produce a 5 Myr record of planktic foraminiferal abundances and a record of stable isotope composition ($\delta^{13}C$) of epibenthic foraminifera from Ocean Drilling Program (ODP) Hole 807A and DSDP Site 214 to constrain the evolution of the WPWP. We compare our results with those from the WEP (ODP Site 806), EEP (ODP Sites 846 and 850), South China Sea (SCS) (ODP Sites 1143, 1147/1148) and a site offshore eastern New Zealand (ODP Site 1125, north slope of Chatham Rise) to explore the spatiotemporal variability of regional paleoceanography. Finally, we discuss the implications of our dataset and analyses to the timing of the IS and the evolution of the WPWP.

3. Materials and Methods

Five hundred eleven core samples were procured from Ocean Drilling Program (ODP) Hole 807A, Leg 130, western Pacific under sample request No. #16790A by AKG for the proposed study. Standard procedures were followed in sample preparation (Gupta and Thomas, 1999, 2003) with necessary precautions to avoid contamination. The sample processing was carried out in the Sample Processing Unit of the Paleoceanography and Paleoclimatology Laboratory, Department of Geology and Geophysics, IIT Kharagpur. The sliced samples were kept in zip lock bags and carefully labelled. 63µm size sieve and a jet of water was used to wash the samples. Contamination was avoided by staining the sieve with methylene blue solution after each wash so that residual microfossils were stained and easily identified. Washed samples were transferred to beakers, and oven dried at ~50º C temperatures. The dried samples were then transferred into glass vials labelled with sample numbers.

3.1 Age Model

The age model used in this study is adopted from the Scientific Reports of ODP Leg 130 (Berggren et al. 1995a, 1995b) based on nannofossil and foraminiferal datums. Age control points are presented in Table 1 and have been updated following the recent geological timescale (Gradstein et al., 2012) (Fig. 3). The age of each sample was interpolated thereby yielding a time resolution of ~20 kyr per sample.

3.2 Sample Analysis: Census counts

271 samples from ODP Hole 807A, western Pacific, and 267 samples from DSDP Site 214, eastern Indian Ocean were used to generate planktic data. Processed samples from ODP Hole 807A were analyzed for mixed-layer species (MLS) of planktic foraminifera. Dry 149 µm+ size fraction was split into suitable aliquots to obtain approximately 300 specimens of planktic foraminifera which were then identified and counted as percentages of overall species (Schmiedl et al., 1997, 2003; den Dulk et al., 1998; Gupta and Thomas, 2003; Gupta et al., 2004).

To investigate changes in the mixed-layer, we used the census counts of MLS which included *Globigerinoides extremus*, *Globigerinoides sacculifer*, *Globigerinoides fistulosus*, *Globigerinoides ruber,* and *Globigerinoides obliquus*. Carbon isotope ($\delta^{13}C$) analyses were performed on epibenthic species *Cibicides wuellerstorfi* and *Cibicides kullenbergi* to understand deep-sea oceanic changes.

3.3 Stable Isotope ($\delta^{13}C$) measurements

Benthic foraminiferal tests were used to measure stable carbon isotope ratios from ODP Hole 807A. 128 samples were analyzed in the Stable Isotope Ratio Mass Spectrometer (Delta V Plus model from Thermo Fisher) Laboratory, Wadia Institute of Himalayan Geology, Dehradun, India. Each sample consisted of 8-10 individuals of benthic foraminifera *Cibicides wuellerstorfi* and *Cibicides kullenbergi* from the >125-micron size fraction. Methanol and subsequent sonification was used to clean the foraminifera to remove unwanted clay and other particles that were present within the test. Benthic foraminifer tests amounting to ~100-300 μg were kept in a sealed glass vial for $\delta^{13}C$ analysis and ultra-pure He gas was introduced to remove the pre-existing gasses. ~99 % orthophosphoric acid was added in the vial to react with the samples for 60 minutes at 72°C. Headspace sampling of released CO_2 was achieved by a double-hole needle connected to a PAL auto-sampler followed by the removal of water by passing it through a Nafion Tube. To remove N_2, in order to collect pure CO_2, the collected gas was released into a Gas Chromatograph (GC) Column through a VALCO system. Subsequently, the purified CO_2 was then introduced in to the Mass Spectrometer for isotopic measurements.

Secondary laboratory standards which were measured against NBS-18 [Value?] were used for day-to-day measurement and to scale all isotope data to Vienna Peedee Belemnite (VPDB). These are Merck Carbonate from Merck ($\delta^{13}C$ = -46.95 ±0.02 ‰ VPDB) and WIHG-STD-2 ($\delta^{13}C$ = -4.9 ±0.01‰ VPDB) prepared from Mussoorie Limestone. The secondary standard was used to check long- term reproducibility as well as inter-laboratory calibration. For the accuracy and consistency of results, a laboratory standard (Merck $CaCO_3$ calibrated against NBS-18) was run several times. Repeat tests and measurements of secondary laboratory standards indicate that the accuracy for carbon and oxygen isotope measurements is better than ~0.1‰ (1SD).

4 Results

Five mixed-layer species of planktic foraminifera were selected to examine paleoceanographic changes in the mixed-layer at Hole 807A. These species are *Globigerinoides extremus*, *Globigerinoides sacculifer, Globigerinoides fistulosus, Globigerinoides ruber* and *Globigerinoides obliquus*. The MLS census data from Hole 807A and Site 214 show a near similar trend during ~3.15 Ma to 1.6 Ma (Fig. 5c). The MLS data shows a gradual increase in their population at both sites 807 and 214 beginning at ~3.6 Ma, with an abrupt increase at ~3.15 Ma. At Hole 807A, the MLS abundances range from 0.3 to a maximum of 31.6% whereas at DSDP Site 214, the MLS population ranges from 1.4 to a maximum of 42.3% with a rapid change occurring at ~2.4 Ma. In contrast to the MLS, *Globigerinita glutinata*, an open-ocean paleoproductivity indicator species [Citation?], shows a drop in its population starting at ~3.15 Ma and continuously decreasing up to ~1.6 Ma, which suggests lowered productivity (Fig. 5a). Over this period, between ~3.15 and 2.1 Ma, the $\delta^{13}C$ of benthic foraminifera decreased from 0.02 to 1.2‰, and also indicate low productivity (Fig. 5b). These results suggest the gradual development of a thick mixed-layer (oligotrophic) and hints at the evolution of the WPWP during the late Pliocene.

5 Discussion

Our data from the western Pacific reveals pronounced changes in the surface-ocean during the Pliocene. The increase in mixed-layer species at Hole 807A suggests the thickening of the mixed-layer (perhaps accompanied by thermocline deepening) in the western Pacific beginning at ~3.15 Ma (Fig. 4). The mixed-layer taxa, in general, are oligotrophic, flourishing in a well-stratified water column and are less abundant in upwelling systems (Brock et al., 1992). Chaisson and Ravelo (2000) linked the formation of the WPWP to a dramatic increase in the Walker Circulation and suggested that the piling of warm surface water by the trade winds made a thicker warm pool after the closure of the IS. The MLS population trend at Hole 807A nearly follows that of DSDP Site 214 between ~3.15 and 1.6 Ma. This suggests that surface-ocean changes at both the sites were near-synchronous and underpins a linkage between the formation of the WPWP and the closure of the IS.

Globigerinita glutinata has a wide latitudinal occurrence, and can tolerate a rather wide range of temperature from 14 to 30°C and 34.4 to 36.4 psu salinities (Bé and Hutson, 1977), and is moderately vulnerable to dissolution. *G. gluntinata* is also known to be found in high abundances in the mid-to-high latitudes as well as in marginal upwelling areas in the low-latitudes (Fairbanks et al., 1982; Thunell and Reynolds, 1984; Pflaumann and Jian, 1999; Kawahata et al., 2002). However, the distribution of *G. glutinata* is mainly linked to the changes in paleoproductivity (Schiebel et al., 2001). According to our dataset, *Globigerinita glutinata* shows an opposite trend as compared to the MLS with a step-wise decrease from ~3.15 to 1.6 Ma at Hole 807A, indicating deepening of the thermocline and/or increased oligotrophic conditions (Fig. 4).

The WPWP was expanded over most parts of the tropics during the early Pliocene. The warm pool then gradually contracted toward the equator (Brierley et al., 2009). To reconstruct the zonal and meridional contraction of the Warm Pool we compared our data with previous work from the EEP, WEP and SCS. Comparing *G. glutinata* abundances and MLS data at Hole 807A with the $\delta^{18}O$ value differences ($\Delta\delta^{18}O$) between *N. dutertrei* (thermocline dweller) and *G. sacculifer* at Site 806, where smaller $\Delta\delta^{18}O$ (*G. sacculifer*- *N. dutertrei*) values at Site 806 suggest deepening of the thermocline under a thickening of the WPWP (Chaisson and Ravelo, 2000), we suggest that thickening of the mixed-layer began at ~3.15 Ma (Fig. 5a, c).

Miller et al. (2012) reported a relatively low sea level between 3.45 and 3.25 Ma. Consequently the ITF decreased significantly, but the heat flow from the Pacific to the Indian

Ocean did not cease completely. However, the Indo-Pacific heat transfer re-established with the major transgression around 3.25 Ma (De Vleeschouwer, D et al., 2019). Our *G. glutinata* data shows an increase in its population beginning at ~3.4 Ma. The increase in its population could be related to the thermocline shoaling in the western Pacific as a result of low sea level. Our MLS data at both the sites suggest that the onset of the modern oligotrophic WPWP occurred at ~3.15 Ma. Prior to ~3.15 Ma we do not see any change in the MLS data at either sites 807 and 214. Weak Walker Circulations (WC) due to the weak zonal SST contrast in the Pacific could be the reason for the disappearance of the warm pool in the western Pacific before ~3.15 Ma (CITE Tierney et al. 2019). We suggest that the warm water shifted slowly in the western Pacific with a gradual reduction in the SST and appearance of Cold Tongue in the EEP since ~3.15 Ma (Fig 5e). The WC intensified with a gradual increase in the equatorial Pacific SST contrast between west pacific and east Pacific. The WC strengthened and pushed warm water to the western Pacific which eventually piled up in the region leading to the establishment of the WPWP.

Comment [KT1]: https://agupubs.onlinelibrary.wiley.com/doi/epdf/10.1029/2019GL083802 - this study supports our idea of weakened WC!

Lawrence et al. (2006) have shown an increase in primary productivity in the eastern Pacific using alkenone concentrations (C_{37} Total) at Site 846. The primary productivity in the EEP is closely linked to the intermediate nutrient-rich cold waters from high latitudes of North and South Pacific. The South Pacific contributes more nutrients to the waters that are upwelled in the EEP (Toggweiler et al., 1991; Sarmiento et al., 2004). The intermediate nutrient rich cold waters from the Southern Ocean high latitudes are transported to the EEP through the EUC (Toggweiler et al., 1991; Bryden & Brady, 1985).

Our results point to a dramatic increase in the EEP primary productivity between ~3 and 1.6 Ma (Fig 5d). The intensification of eastern Pacific upwelling cell has been related to the gradual development of the zonal SST gradients at this time (Steph et al., 2010; Tierney et al. 2019). Our MLS population abundances at both Sites 807 and 214 are tightly synchronous with the primary production in the EEP (Fig 5c). The SST data from Zhang et al. (2014) at Site 850 and Herbert et al. (2016) at Site 846 from EEP also show a gradual decrease in the SST at the same time which indicates thermocline shoaling and appearance of the CT in the EEP at about ~3.15 Ma (Fig 5e). The northward drift of Australia, which restricted the ITF, could have led to the global oceanic thermocline shoaling at about 3 Ma (Cane and Molnar, 2001).

We propose that the zonal migration of equatorial Pacific Warm water from east to west started with a gradual decrease in SST and with an appearance of CT in the EEP. These processes eventually strengthened the WC and tectonic forcing gradually constricted the IS and restricted ITF strength, thereby strengthening the WPWP. Data from the South China Sea (SCS) show a reduction in SSTs at ~ 3 Ma at ODP Sites 1147 and 1148 (Jia et al., 2008) at the edge of the warm pool, whereas at ODP Site 1143 the SST remained relatively stable (Li et al., 2011). Prior to ~3 Ma, the SST was similar at both the sites. Further, data from the SCS suggests the contraction of the WPWP towards the equator i.e. towards ODP Hole 807A in the late Pliocene (Fig. 5g). SST U^{k}_{37} data from ODP Site 1125 (Fedorov et al., 2015) also shows a fall in SST at ~3.15 Ma, suggesting narrowing of the expanded warm pool towards the equator from the southern ocean during this time (Fig. 5f).

6. Conclusions

The evolutionary record of the West Pacific Warm Pool (WPWP) was reconstructed using foraminiferal abundances and their isotopic signatures at ODP Hole 807A and DSDP Site 214 in the western equatorial Pacific Ocean and eastern Indian Ocean, respectively. We find a stark decrease in productivity and increase in mixed-layer thickness beginning around 3.15 Ma at the study sites, suggesting that such surface oceanographic changes were linked to the development of the Indo-Pacific warm pool. Our findings support previously published work and provide further evidence for the evolution of the Indo-Pacific warm pool during the late Pliocene. We conclude that evolution of the Indo-Pacific warm Pool was closely linked to progressive narrowing of the Indonesian seaway. Such a tectono-oceanic change may have had far-reaching impact on the Asia-African climate regime that might have contributed to the future course of human evolution.

Acknowledgements

We would like to thank Ocean Drilling Program for providing samples (No. #16790A). We are grateful to Wadia Institute of Himalayan Geology for providing the Stable isotope facility for this study and IIT Kharagpur for laboratory facilities to carry out this work. AKG thanks the DST, Government of India, New Delhi for Sir J.C. Bose Fellowship (No. SR/S2/JCB-80/2011). The data has been uploaded on Zonodo.org

(DOI: https://doi.org/10.5281/zenodo.3631160)

References

Auer, G., De Vleeschouwer, D., Smith, R. A., Bogus, K., Groeneveld, J., Grunert, P., & Gallagher, S. J. (2019). Timing and pacing of Indonesian Throughflow restriction and its connection to Late Pliocene climate shifts. Paleoceanography and Paleoclimatology, 34(4), 635-657.

Be´, A. W. (1977). An ecological, zoogeographic and taxonomic review of recent planktic foraminifera. *Oceanic micropaleontology*, *1*, 1-100.

Berggren, W. A., Hilgen, F. J., Langereis, C. G., Kent, D. V., Obradivich, J. D., Raffi, I., Raymo, M. E., Shackleton, N. J. (1995a). Late Neogene chronology: New perspectives in high resolution stratigraphy, Geological Society of American Bulletin, Vol. 107, pp. 1272-1287.

Berggren, W. A., Kent, D. V., Swisher, C. C. III, Aubry, M.-P. (1995b). A revised Cenozoic geochronology and chronostratigraphy, by Berggren, W. A. (Ed.) Geochronology, Time scale and Global Stratigraphic Correlation, The Society of Economic Paleontologists and Mineralogists Special Publication, Vol. 54, pp. 129- 212.

Brierley, C. M., Fedorov, A. V., Liu, Z., Herbert, T. D., Lawrence, K. T., & LaRiviere, J. P. (2009). Greatly expanded tropical warm pool and weakened Hadley circulation in the early Pliocene. Science, 323(5922), 1714-1718.

Bryden, H. L., & Brady, E. C. (1985). Diagnostic model of the three-dimensional circulation in the upper equatorial Pacific Ocean. Journal of Physical Oceanography, 15(10), 1255–1273. https://doi.org/10.1175/1520-0485(1985)015<1255:DMOTTD>2.0.CO;2

Brock, J.C., McClain, C.R., Anderson, D.M., Prell, W.L. & Hay, W.W. (1992). Southwest monsoon circulation and environments of recent planktic foraminifera in the northwestern Arabian Sea. Paleoceanography, 7(6): 799-813.

Cane, M. A., & Molnar, P. (2001). Closing of the Indonesian seaway as a precursor to east African aridification around 3–4 million years ago. Nature, 411(6834), 157-162.

Cannariato, K. G., & Ravelo, A. C. (1997). Pliocene-Pleistocene evolution of eastern tropical Pacific surface water circulation and thermocline depth. Paleoceanography, 12(6), 805-820

Chaisson, W.P. (1995). Planktic foraminiferal assemblages and paleoceanographic change in the trans-tropical Pacific Ocean: A comparison of west (Leg 130) and east (Leg 138), latest Miocene to Pleistocene. Proceedings of the Ocean Drilling Program, Scientific Results, 138, pp. 555-597.

Chaisson, W. P., & Ravelo, A. C. (2000). Pliocene development of the east-west hydrographic gradient in the equatorial Pacific. Paleoceanography, 15(5), 497-505.

Chong, J. C., J. Sprintall, S. Hautala, W. L. Morawitz, N. A. Bray, and W. Pandoe (2000). Shallow throughflow variability in the outflow straits of Indonesia, Geophys. Res. Lett., 27, 125–128.

De Garidel-Thoron, T., Rosenthal, Y., Bassinot, F., Beaufort, L. (2005). Stable sea surface temperatures in the western Pacific warm pool over the past 1.75 million years. Nature 433, 294–298.

den Dulk, M., Reichert, G. J., Memon, G. M., Roelofs, E. M., Zachariasse, W. J., Van der Zwaan, G. J. (1998). Benthic foraminiferal response to variation in surface water productivity and oxygenation in the northern Arabian Sea, *Marine Micropaleonotology*, Vol. 35, pp. 43-66.

Drenkard, E. J., & Karnauskas, K. B. (2014). Strengthening of the Pacific equatorial undercurrent in the SODA reanalysis: Mechanisms, ocean dynamics, and implications. Journal of Climate, 27(6), 2405-2416.

Fairbanks, R. G., Sverdlove, M., Free, R., Wiebe, P. H., and Be´, A. W. H. (1982). Vertical distribution and isotopic fractionation of living planktic foraminifera from the Panama Basin. Nature, Vol. 298, pp. 841-844.

Fedorov, A. V., Burls, N. J., Lawrence, K. T., & Peterson, L. C. (2015). Tightly linked zonal and meridional sea surface temperature gradients over the past five million years. Nature Geoscience, 8(12), 975.

Ganachaud, A., and C. Wunsch (2000), Improved estimates of global ocean circulation, heat transport and mixing from hydrographic data, Nature, 408, 453– 457.

Gordon, A. L., & Fine, R. A. (1996). Pathways of water between the Pacific and Indian oceans in the Indonesian seas. Nature, 379(6561), 146.

Gordon, A. L., Susanto, R. D., & Ffield, A. (1999). Throughflow within Makassar Strait. Geophysical Research Letters, 26(21), 3325-3328.

Gradstein, F.M., Ogg, J.G., Schmitz, M.D., and Ogg, G.M., eds (2012) The Geological Time Scale 2012, Amsterdam, Elsevier, 2 vols., 1144 p.

Gupta, A.K. and Thomas, E., (1999). Latest Miocene-Pleistocene productivity and deep-sea ventilation in the northwestern Indian Ocean (DSDP Site 219). Paleoceanography, 14, 62-73.

Gupta, A. K., and Thomas, E. (2003). Initiation of Northern Hemisphere Glaciation and strengthening of the northeast Indian monsoon: Ocean Drilling Program site 758, eastern equatorial Indian Ocean. Geology, Vol. 31, pp. 47-50.

Herbert, T. D., Lawrence, K. T., Tzanova, A., Peterson, L. C., Caballero-Gill, R., & Kelly, C. S. (2016). Late Miocene global cooling and the rise of modern ecosystems. Nature Geoscience, 9(11), 843.

Jia, G., Chen, F., & Peng, P. A. (2008). Sea surface temperature differences between the western equatorial Pacific and northern South China Sea since the Pliocene and their paleoclimatic implications. Geophysical Research Letters, 35(18).

Jian, Z., Yu, Y., Li, B., Wang, J., Zhang, X., Zhou, Z. (2006). Phased evolution of the south–north hydrographic gradient in the South China Sea since the middle Miocene. Palaeogeography, Palaeoclimatology, Palaeoecology 230, 251–263.

Karnauskas, K. B., & Cohen, A. L. (2012). Equatorial refuge amid tropical warming. Nature Climate Change, 2(7), 530.

Kawahata, H., Nishimura, A., and Gagan, M. K. (2002). Seasonal change in foraminiferal production in the western equatorial Pacific warm pool: evidence from sediment trap experiments. Deep-Sea Research II, Vol. 49, pp. 2783-2800.

Keller, G. (1985). Depth stratification of planktic foraminifers in the Miocene ocean. Geological Society of America Memoirs, 163, 177-196.

Kennett, J. P., G. Keller, and M. S. Srinivasan, (1985). Miocene planktic foraminiferal biogeography and paleogeographic development of the Indo-Pacific region, in The Miocene Ocean: Paleoceanography and Biogeography, edited by J. P. Kennett, pp. 197–236.

Lawrence, K. T., Liu, Z., & Herbert, T. D. (2006). Evolution of the eastern tropical Pacific through Plio-Pleistocene glaciation. Science, 312(5770), 79-83.

Li, L., Li, Q., Tian, J., Wang, P., Wang, H., & Liu, Z. (2011). A 4-Ma record of thermal evolution in the tropical western Pacific and its implications on climate change. Earth and Planetary Science Letters, 309(1), 10-20.

Li, Q., Li, B., Zhong, G., McGowran, B., Zhou, Z., Wang, J., Wang, P. (2006). Late Miocene development of the western Pacific warm pool: planktic foraminifer and oxygen isotopic evidence. Palaeogeography, Palaeoclimatology, Palaeoecology 237, 465–482.

Linsley, B. K., Rosenthal, Y., & Oppo, D. W. (2010). Holocene evolution of the Indonesian throughflow and the western Pacific warm pool. Nature Geoscience, 3(8), 578.

Meyers, G. (1996). Variations of Indonesian throughflow and El Niño - Southern Oscillation, J. Geophys. Res., 101(C5), 12255–12263.

Miller, K. G., Wright, J. D., Browning, J. V., Kulpecz, A., Kominz, M., Naish, T. R., ... & Sosdian, S. (2012). High tide of the warm Pliocene: Implications of global sea level for Antarctic deglaciation. Geology, 40(5), 407-410.

Nathan, S. A., & Leckie, R. M. (2009). Early history of the Western Pacific Warm Pool during the middle to late Miocene (~ 13.2–5.8 Ma): Role of sea-level change and implications for equatorial circulation. Palaeogeography, Palaeoclimatology, Palaeoecology, 274(3-4), 140-159.

Pflaumann, U., & Jian, Z. (1999). Modern distribution patterns of planktonic foraminifera in the South China Sea and western Pacific: a new transfer technique to estimate regional sea-surface temperatures. Marine Geology, 156(1-4), 41-83.

Ravelo, A. C., Dekens, P. S., & McCarthy, M. (2006). Evidence for El Niño-like conditions during the Pliocene. GSA today, 16(3), 4-11.

Ryan, J. P., Ueki, I., Chao, Y., Zhang, H., Polito, P. S., & Chavez, F. P. (2006). Western Pacific modulation of large phytoplankton blooms in the central and eastern equatorial Pacific. Journal of Geophysical Research: Biogeosciences, 111(G2).

Sarmiento, J. L., Gruber, N., Brzezinski, M. A., & Dunne, J. P. (2004). High-latitude controls of thermocline nutrients and low latitude biological productivity. Nature, 427(6969), 56.

Sato, K., Oda, M., Chiyonobu, S., Kimoto, K., Domitsu, H., & Ingle, J. C. (2008). Establishment of the western Pacific warm pool during the Pliocene: Evidence from planktic foraminifera, oxygen isotopes, and Mg/Ca ratios. Palaeogeography, Palaeoclimatology, Palaeoecology, 265(1), 140-147.

Schiebel, R., Waniek, J., Bork, M., and Hemleben, C. (2001). Planktic foraminiferal production stimulated by chlorophyll redistribution and entrainment of nutrients. Deep Sea Research Part I: Oceanographic Research Papers, 48(3), 721-740.

Schlitzer, R., Ocean Data View, http://odv.awi.de, 2014.

Schmiedl, G., Mackensen, A. and Muller, P.J. (1997). Recent benthic foraminifera from the eastern South Atlantic Ocean: Dependence on food supply and water masses. Marine Micropaleontology, 32, pp. 249-287.

Schmiedl, G., Mitschele, A., Beck, S., Emeis, K. -C., Hemleben, C., Schulz, H., Sperling, M., Weldeab, S. (2003). Benthic foraminiferal record of ecosystem variability in the eastern Mediterranean Sea during the times of sapropel S5 and S6, Palaeogeography, Palaeoclimatology, Palaeoecology, Vol. 190, pp. 139-164.

Schott, F. A, and J. P. McCreary, (2001). The monsoon circulation of the Indian Ocean, Progress Oceanogr., 51, 1–123.

Steph, S., Tiedemann, R., Prange, M., Groeneveld, J., Schulz, M., Timmermann, A., ... & Haug, G. H. (2010). Early Pliocene increase in thermohaline overturning: A precondition for the development of the modern equatorial Pacific cold tongue. Paleoceanography, 25(2).

Sun, D. Z. (2003), Possible effect of an increase in the warm-pool SST on the magnitude of El Niño warming, J. Clim., 16, 185–205.

Thunell, R. C., & Reynolds, L. A. (1984). Sedimentation of planktic foraminifera: seasonal changes in species flux in the Panama Basin. Micropaleontology, 243-262.

Toggweiler, J. R., Dixon, K., & Broecker, W. S. (1991). The Peru upwelling and the ventilation of the South Pacific thermocline. Journal of Geophysical Research: Oceans, 96(C11), 20467-20497.

Vranes, K., Gordon, A. L., & Ffield, A. (2002). The heat transport of the Indonesian Throughflow and implications for the Indian Ocean heat budget. Deep Sea Research Part II: Topical Studies in Oceanography, 49(7-8), 1391-1410.

Webster, P.J., Palmer, T.N. (1997). The past and future of El Niño. Nature 390, 562–564.

Wyrtki, K., & Kilonsky, B. (1984). Mean water and current structure during the Hawaii-to-Tahiti shuttle experiment. Journal of Physical Oceanography, 14(2), 242-254.

Yan, X. H., Ho, C. R., Zheng, Q., & Klemas, V. (1992). Temperature and size variabilities of the Western Pacific Warm Pool. Science, 258(5088), 1643-1646.

Zhang, Y. G., Pagani, M., & Liu, Z. (2014). A 12-million-year temperature history of the tropical Pacific Ocean. Science, 344(6179), 84-87.

Figure captions:

Figure 1: Location of ODP Hole 807A and DSDP Site 214. Background was created using Ocean-Data-View (Schlitzer, 2014). NEC = North Equatorial Current; NECC = North Equatorial Countercurrent; SEC = South Equatorial Current, SECC = South Equatorial

Countercurrent; EUC = Equatorial Undercurrent; MC = Mindanao Current; ME = Mindanao Eddy; HE = Halmahera Eddy.

Figure 2: Average ocean surface temperature along the equator in the Pacific. Background was created using Ocean-Data-View (Schlitzer, 2014).

Figure 3: Depth vs Age plot at ODP Hole 807A based on foraminiferal and nannofossil datums (Gradstein et al., 2012).

Figure 4: Percent distribution of *Globorotalia glutinata* (a) and mixed-layer species (b) at ODP Hole 807A.

Figure 5: Proxy records at ODP Hole 807A compared with those from the other sites. (a) Percentage distribution of *Globigerinita glutinata* (present study) and The $\delta^{18}O$ differences ($\Delta\delta^{18}O$ values) between *Globigerinoides sacculifer* (surface) and *Neogloboquadrina dutertrei* (thermocline) dwellers at ODP Site 806 (Chaisson and Ravelo, 2000) (red), (b) $\delta^{13}C$ values of *Cibicides wuellerstorfi* and *Cibicides kullenbergi* at ODP Hole 807A present study), (c) % Mixed-layer species at ODP Hole 807A and DSDP Site 214 (present study), (d) Concentration of alkenones C_{37} Total (nmol/g) at ODP Site 846 (Lawrence et al., 2006). (e) SST based on U^k_{37} at ODP Site 138-846 U^k_{37} (Herbert, TD et al., 2016) (green) and SST based on TEX_{86} at ODP 850 (Zhang et al., 2014) (red), (f) SST based on U^k_{37} at ODP Site 1125 (Fedorov et al., 2015), (g) SST based on U^k_{37} at ODP Site 1143 (Li et al., 2011) and at ODP Site 1147/1148 (Jia et al., 2008). IG = Indonesian Gateway; WPWP = West Pacific Warm Pool; MPWP = Mid-Pliocene Warm Period.

Table 1: The calcareous nannofossil and foraminiferal datums from ODP Hole 807A with their ages from Berggren et al. (1995a, 1995b) and updated to Gradstein et al. (2012).

Datum	Events	Depth	GTS 2012
LAD	*P.lacunosa (N)*	12.15	0.44
LAD	*C.macintyrei (N)*	21.65	1.6
LAD	*G.fistulosus (F)*	31.15	1.88

FAD	*G.truncatulinoides (F)*	31.15	1.93
LAD	*D.tamalis (N)*	40.65	2.8
LAD	*G.altispira (F)*	59.65	3.13
FAD	*G.fistulosus (F)*	69.15	3.33
LAD	*C.acutus (N)*	88.15	5.04

Figure 1.

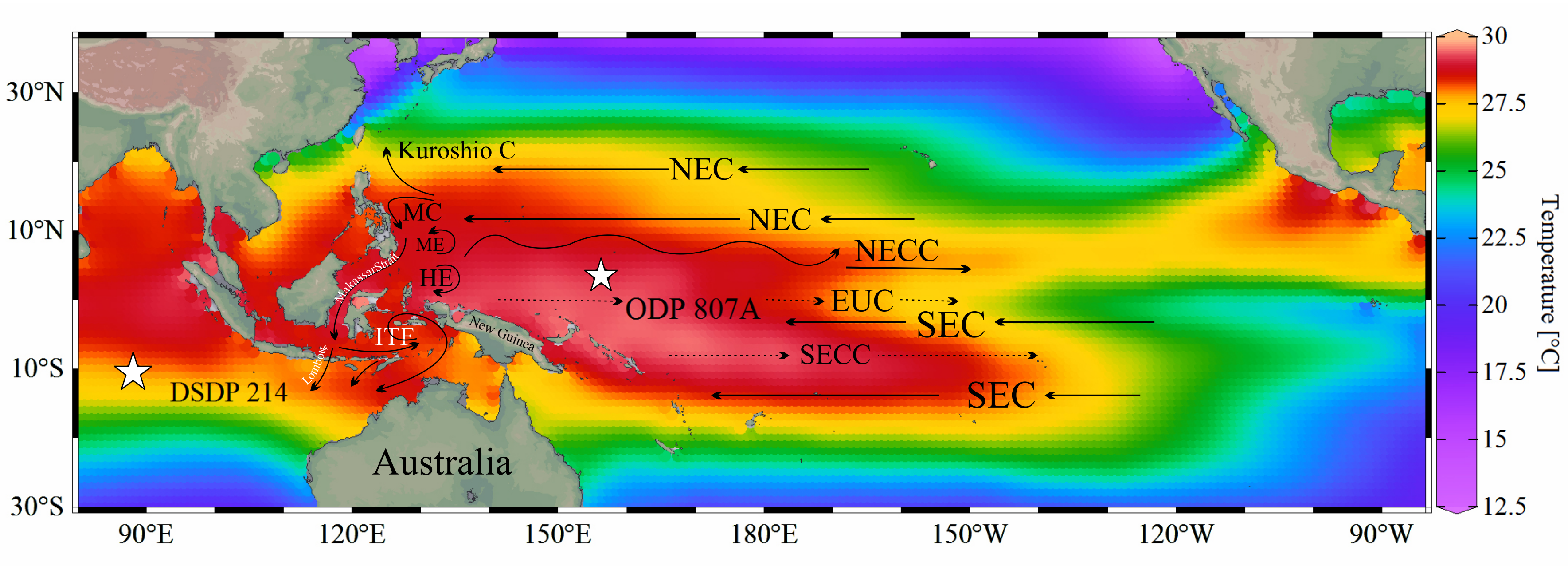

Figure 1: Location of ODP Hole 807A and DSDP Site 214. Background was created using Ocean-Data-View (Schlitzer, 2014). NEC = North Equatorial Current; NECC = North Equatorial Countercurrent; SEC = South Equatorial Current, SECC = South Equatorial Countercurrent; EUC = Equatorial Undercurrent; MC = Mindanao Current; ME = Mindanao Eddy; HE = Halmahera Eddy.

Figure 2.

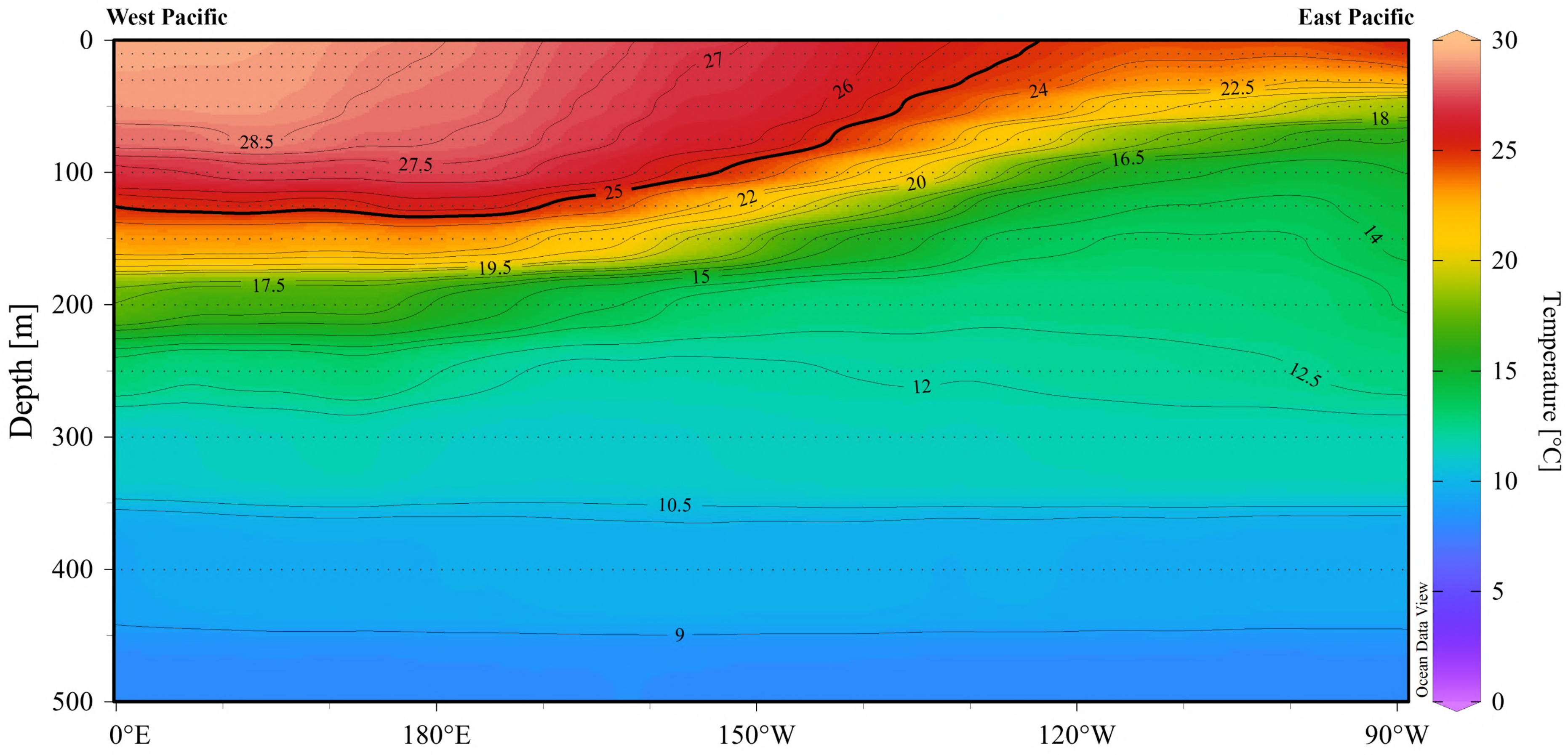

Figure 2: Average ocean surface temperature along the equator in the Pacific.
Background was created using Ocean-Data-View (Schlitzer, 2014).

Figure 3.

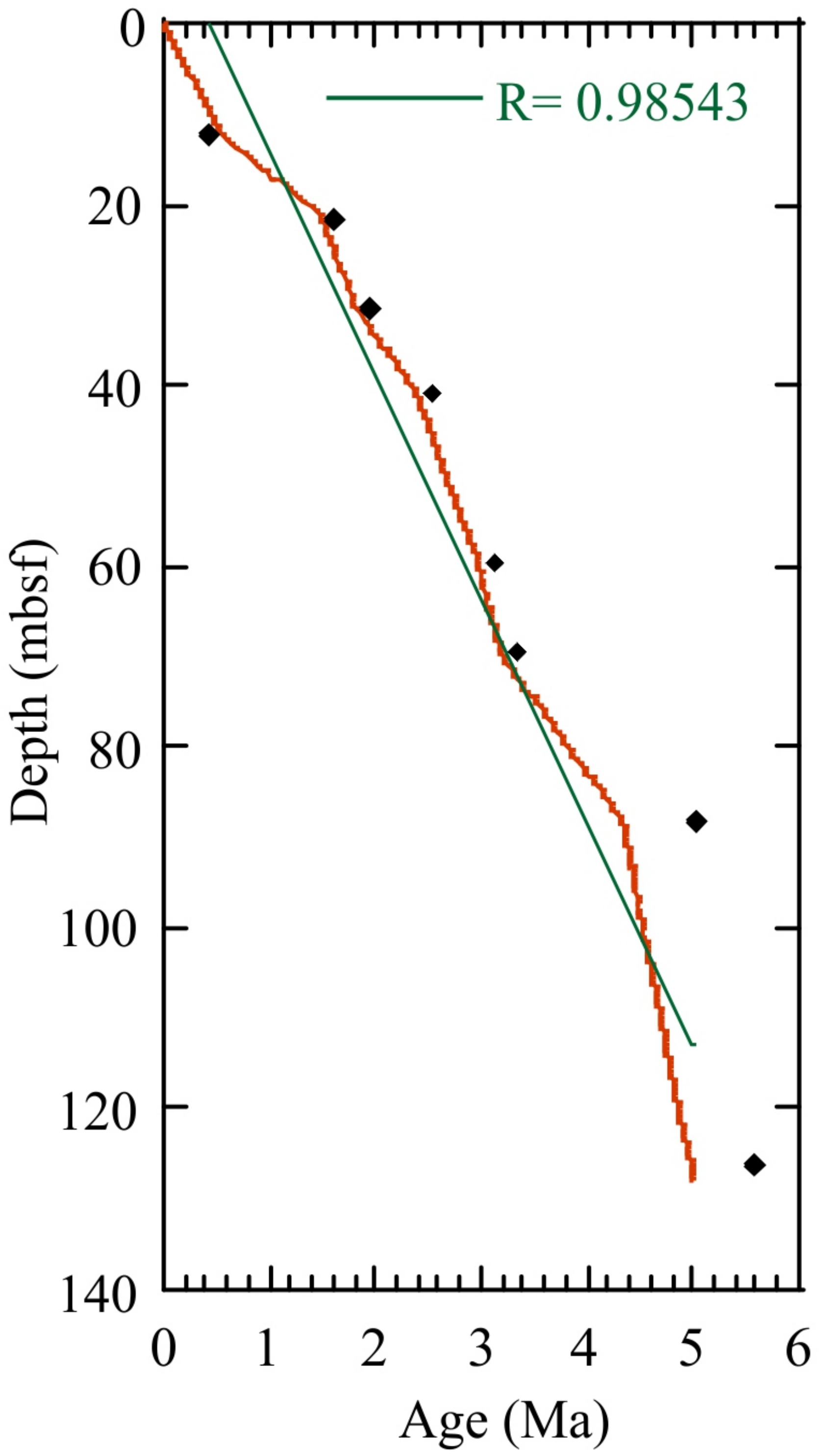

Figure 3: Depth vs Age plot at ODP Hole 807A based on foraminiferal and nannofossil datums (Gradstein et al., 2012).

Figure 4.

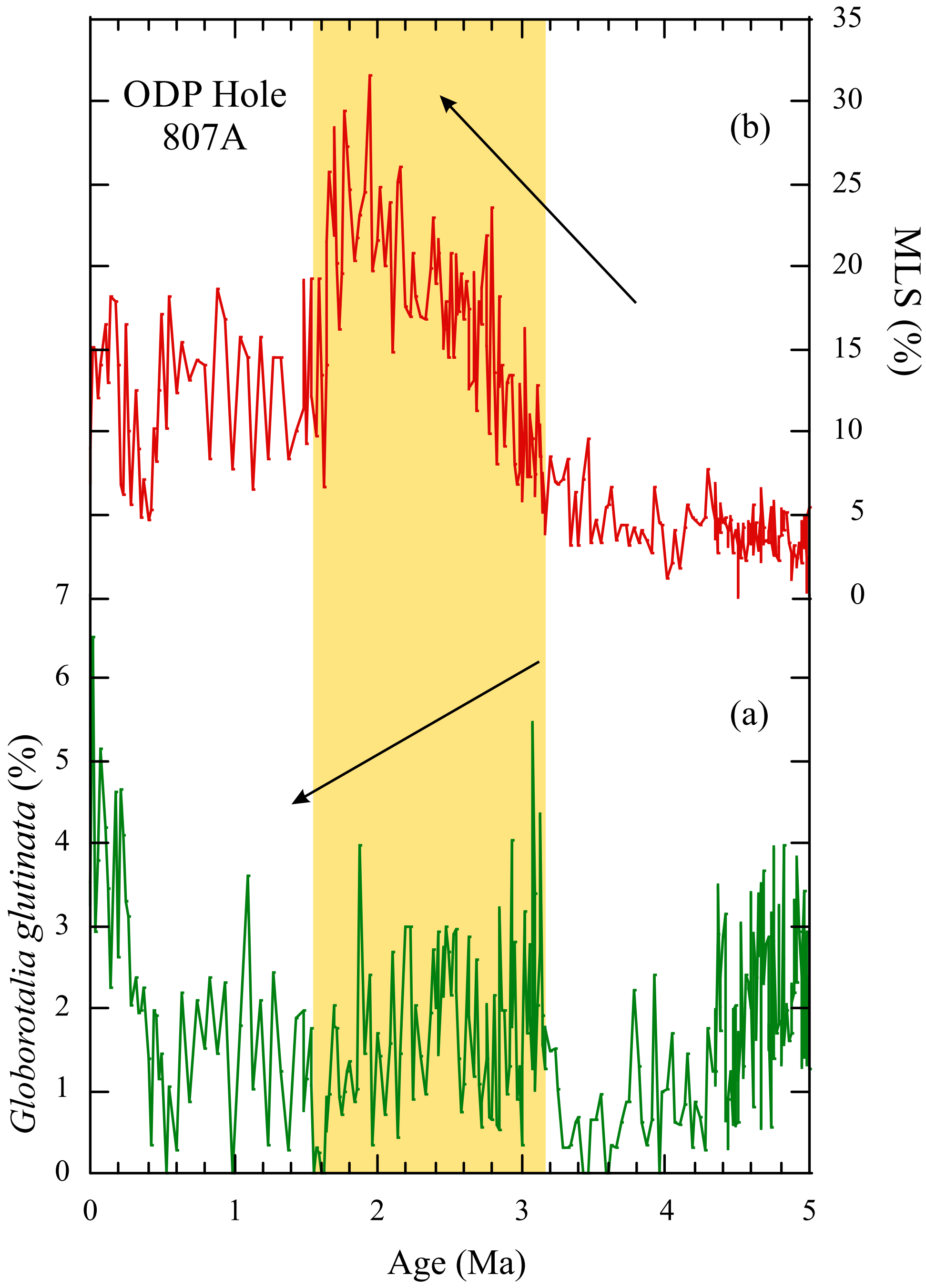

Figure 4: Percentage distribution of *Globorotalia glutinata* (a), % Mixed layer Species (b) at ODP Hole 807A.

Figure 5.

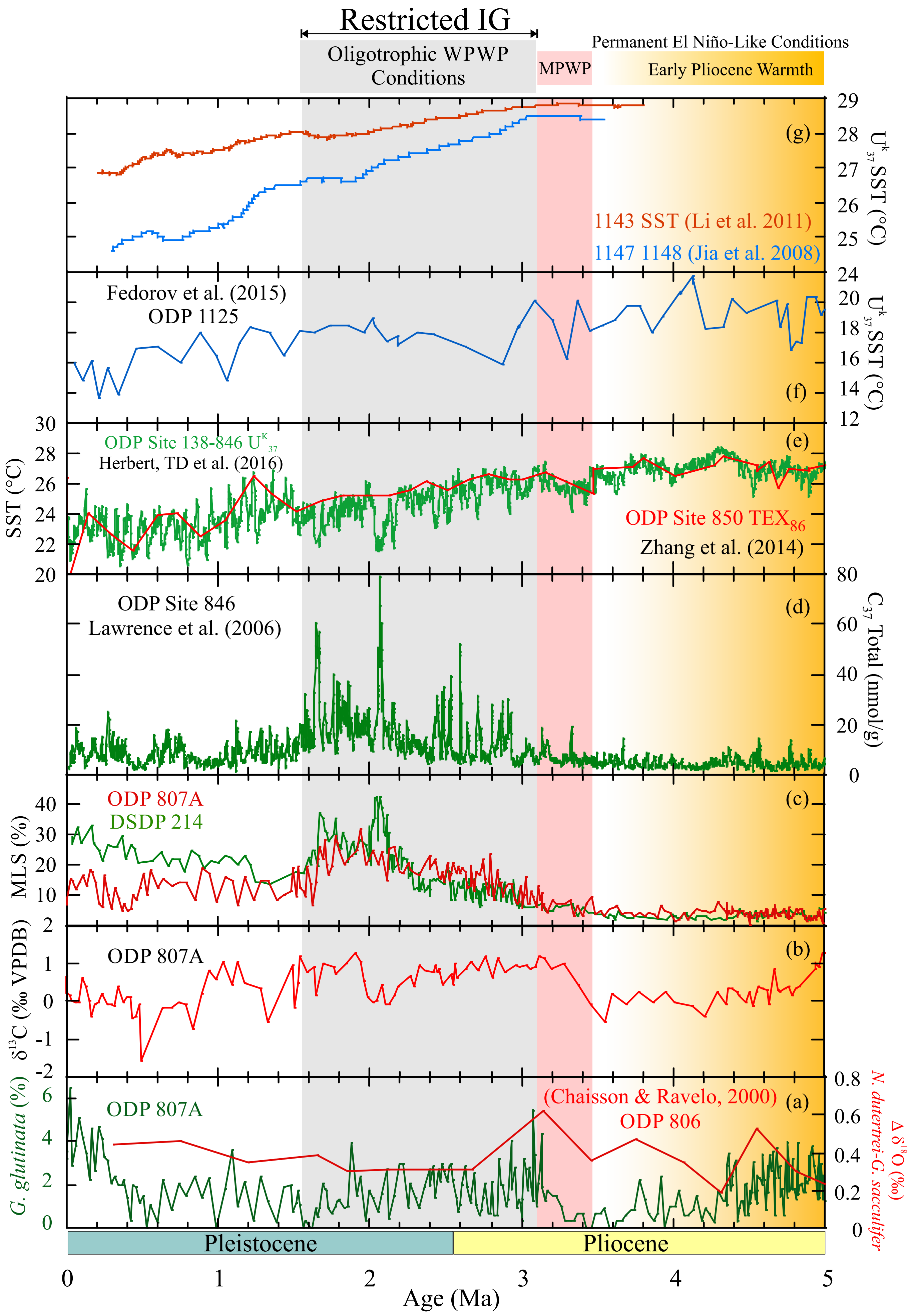

Figure 5: Proxy records at ODP Hole 807A compared with those from the other sites. (a) Percentage distribution of *Globigerinita glutinata* (present study) and The $\delta^{18}O$ differences ($\Delta\delta^{18}O$ values) between *Globigerinoides sacculifer* (surface) and *Neogloboquadrina dutertrei* (thermocline) dwellers at ODP Site 806 (Chaisson and Ravelo, 2000) (red), (b) $\delta^{13}C$ values of *Cibicides wuellerstorfi* and *Cibicides kullenbergi* at ODP Hole 807A present study), (c) % Mixed-layer species at ODP Hole 807A and DSDP Site 214 (present study), (d) Concentration of alkenones C_{37} Total (nmol/g) at ODP Site 846 (Lawrence et al., 2006). (e) SST based on U^{k}_{37} at ODP Site 138-846 U^{k}_{37} (Herbert, TD et al., 2016) (green) and SST based on TEX_{86} at ODP 850 (Zhang et al., 2014) (red), (f) SST based on U^{k}_{37} at ODP Site 1125 (Fedorov et al., 2015), (g) SST based on U^{k}_{37} at ODP Site 1143 (Li et al., 2011) and at ODP Site 1147/1148 (Jia et al., 2008). IG = Indonesian Gateway; WPWP = West Pacific Warm Pool; MPWP = Mid-Pliocene Warm Period.